



Enhanced performance of a single-chamber solid oxide fuel cell with dual gas supply method

Yanting Tian¹ · Zhe Lü² · Zhihong Wang² · Bo Wei² · Zhongquan Nie¹ · Aiping Zhai¹

Received: 28 September 2018 / Revised: 24 January 2019 / Accepted: 25 January 2019 / Published online: 7 February 2019
© Springer-Verlag GmbH Germany, part of Springer Nature 2019

Abstract

Single-chamber solid oxide fuel cell made of conventional materials with two gas tubes located at the different sides of the cell was fabricated and tested in a diluted methane-oxygen mixture to evaluate the influence of various operating parameters on cell performance. The traditional gas supply method was also studied for comparison. Experimental results showed that the cell performance was greatly enhanced by using the dual gas supply method. At a furnace temperature of 700 °C, the maximum power density was 459.2 mW cm⁻² for a CH₄/O₂ ratio of 1.5, which was 67% higher than that of the traditional gas supply method. Additionally, the dual gas supply method could provide the required reactant gas for each electrode by changing the gas composition of both the gas tubes separately. The highest power density of 493.9 mW cm⁻² was obtained at the anode and cathode CH₄/O₂ ratios of 1.5 and 1, respectively. A cell with dual gas supply method will generate a more attractive power output than that of the traditional method in a single-chamber condition.

Keywords Single-chamber solid oxide fuel cell · Dual gas supply method · Flow geometry · CH₄/O₂ ratio

Introduction

Solid oxide fuel cells (SOFCs) are devices for electrochemically converting the chemical energy of the fuel gas into electrical energy in an environment friendly way with high efficiency [1, 2]. Because of their high operation temperature, a wide range of hydrocarbon fuels can be easily reformed within the cell, promotes rapid electro-catalysis with nonprecious metals [3–6]. However, the necessity of gas separation and sealing has a severe impact on the mechanical and thermal shock resistance of SOFCs and their long-term stability. In comparison to the conventional SOFCs, both the anode and cathode of single-chamber SOFCs (SC-SOFCs) are exposed to the same mixture of fuel and oxygen. Therefore, SC-SOFCs are more shock resistant, both thermally and mechanically,

according to the eliminating of sealing processes [7, 8]. The operation mechanism of SC-SOFCs is based on the selective properties of the anode and cathode towards the fuel/oxygen mixture [9–11]. The ideal anode should catalyze the partial oxidation of hydrocarbon to H₂ and CO, which are further oxidized to H₂O and CO₂, respectively. Typical oxidation reactions using methane are



The ideal cathode should catalyze the reduction of oxygen, thus generating an electromotive force between the electrodes [12, 13]. The equation at the cathode is given as following



Up to now, researches are mainly focused on the investigation of the operating parameters, such as the fuel types [14–16], fuel to oxygen ratio [17–19], gas flow rate [9, 20, 21], the heat released by the combustion reactions [22, 23], and electrode materials of SC-SOFCs [24, 25]. The flow geometry is also important in determining the cell performance.

✉ Yanting Tian
yanting_005@163.com

✉ Zhe Lü
lvzhe@hit.edu.cn

¹ College of Physics and Optoelectronics, Taiyuan University of Technology, Taiyuan 030024, China

² Department of Physics, Harbin Institute of Technology, Harbin 150001, China

Bay et al. [26] showed that the different cell performances between the chamber configuration designs for SC-SOFCs were due to the different gas flow around the cell. To date, however, few discussions have really tackled the subject of the gas flow geometry on the performance of SC-SOFCs. According to Stefan et al. [27], the strong influence of flow geometry was due to its effect on gas composition, particularly on the oxygen chemical potential at the two electrodes as a result of gas mixing. The chamber design with the cathode first configuration yielded the best performance at lower flow rates, while the open tube design with the electrodes equally exposed to the inlet gas worked best at higher flow rates. Morel et al. [28] have reported that the electrolyte-supported SC-SOFCs with smaller cathodes positioned on the opposite side of a full-size anode always perform better when the cathodes were located at the inlet position. Jacques-Bedard et al. [29] tested different configurations of the cell with coplanar interdigitated electrodes located on the same side of the electrolyte, where the cell configuration was determined by the electrodes positioning in regard to the gas flow. The lowest performance obtained in the cell configuration with the anode exposed to the gas flow, which was explained by the promotion of the oxygen consumption before the gas mixture reaches the cathode.

Based on these investigations, the relative positioning of the electrodes in regard to the incoming gas flow exerts a significant influence on the performance of a SC-SOFC as the gas composition is modified through the catalytic oxidation of the fuel over the anode. This concern is also important for stacked cells where the downstream cells are exposed to the gas composition modified by fuel oxidation of the upstream cells. In our previous study of a SC-SOFC microstack [30], a novel gas supply method with separated gas vents in the gas tube was proposed. Results showed that the single cells could obtain a more uniform gas distribution by using the separated gas supply method. This novel way of gas supply mode effectively refined the distribution of gas flow geometry around the cells and thus produced a better performance.

In the present paper, we are thus continuing our investigation of gas supply method with small gas vent arranged at the side of gas tube for the reactant gas flow to the electrodes. Two gas tubes were used to transmit gas mixture of methane and oxygen for anode and cathode separately. Therefore, each electrode could obtain required gas composition by its own gas tube. The traditional gas supply method was also investigated for comparison.

Experimental

The single cells were purchased from Ningbo Institute of Material Technology & Engineering, Chinese Academy of

Sciences. A conventional NiO/yttria-stabilized zirconia (YSZ) anode was fabricated using the tape casting method as the support of the SOFC. The YSZ electrolyte films with a thickness of 8 μm were prepared by spraying method. Conventional cathode material, $(\text{La}_{0.75}\text{Sr}_{0.25})_{0.95}\text{MnO}_3$ (LSM), was then coated onto the YSZ films and the thickness of the LSM cathode was 25 μm . The size of the cells was $1 \times 1 \text{ cm}^2$, and the active cathode area of each cell was $0.7 \times 0.7 \text{ cm}^2$. The schematic diagram of the cell configuration is shown in Fig. 1a. Prior to cell assembly, NiO in anode substrate was reduced to metallic Ni in hydrogen atmosphere using a dual-chamber configuration at 700 $^\circ\text{C}$. The anode was fed hydrogen while the cathode was exposed to air in order to avoid the reduction of cathodes [31, 32].

The performance of the cell was tested in a quartz tube, as shown in Fig. 1b. The inner and outer diameter of the quartz tube was 17.5 and 20.7 mm, respectively. The cell was assembled in a piece of lightweight dichroite ceramic board with many square holes. In order to fix the cell in place, the surface of the ceramic board was fluted [32, 33]. Two half-open ceramic tubes, each with an inner and outer diameter of 2 and

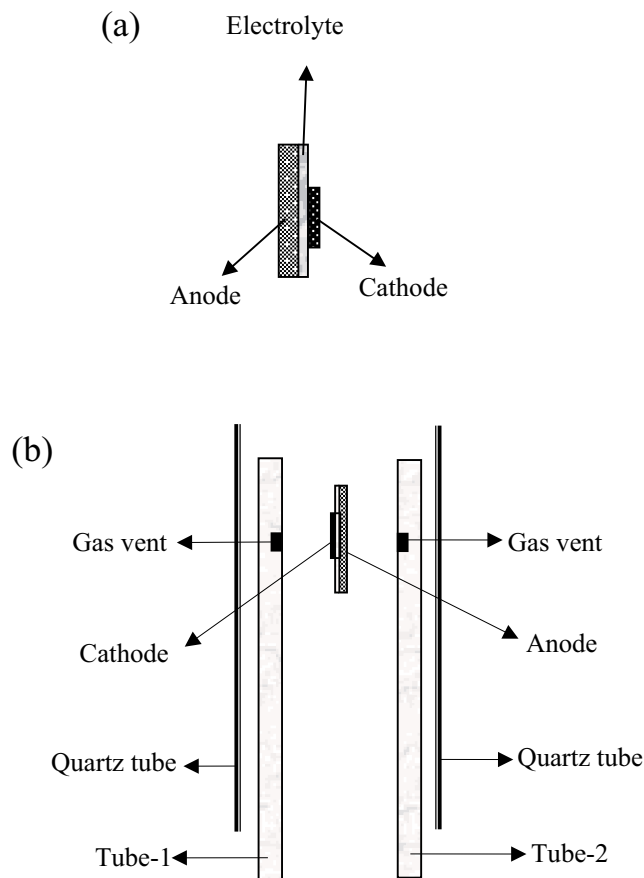


Fig. 1 The schematic diagram of the cell and the gas supply configuration: **a** single-cell and **b** dual-gas supply configuration. Figure 1 was performed with the drawing function of MSOffice, Fig. 4 was the SEM image, and the rest of the images were performed with the graphic program of Origin 8.0

3.4 mm, were used to transport the reactant gas consisting of nitrogen, methane, and oxygen. Small gas vents were arranged at the side of the gas tubes for the reactant gas flow to the electrodes. The tube arranged at the cathode side was marked as tube 1, and the one at the anode side was marked as tube 2.

The flow rates of nitrogen, methane, and oxygen were controlled by mass-flow controllers (MFCs, D08-4D/2M, Seven-Star Huachuang, China). The cell was measured by a BiStat potentiostat (VSP, Bio-logic SAS) at a furnace temperature of 700 °C. Silver paste (DAD-87, Shanghai Research Institute of Synthetic Resin, China) was painted onto the electrode surface as the current collector and the cells were connected to the test instruments using silver wires. Scanning electron microscopy (SEM, FEI Quanta 200F) was used to characterize the morphology and microstructure of the cells.

Results and discussion

The performance of the cell operated under traditional gas supply method was tested in CH₄-O₂-N₂ mixtures at 700 °C. Figure 2 shows the current-voltage (*I-V*) and current-power (*I-P*) curves of the cell under various CH₄/O₂ ratios (*R*). The flow rate of N₂ was fixed at 200 sccm and the total flow rate of CH₄ and O₂ was 200 sccm. An increase of the open-circuit voltage (OCV) occurred with increasing CH₄/O₂ ratios and the OCV at *R* = 2 was 1 V. The maximum power densities of 244.9, 275.5, and 255.1 mW cm⁻² were obtained at *R* = 1, 1.5, and 2, respectively. The *I-V* curve of the cell exhibited obvious concentration polarization at high current at *R* = 1, which led to a degradation of the cell performance.

The cell owned a cathode-first and an anode-first configuration when tube 1 and tube 2 were used as the gas transmission path, respectively. Unlike the traditional gas supply method, the gas vents of the gas tubes were located at the side of the cell for the reactant gas flow to the electrodes. Figure 3

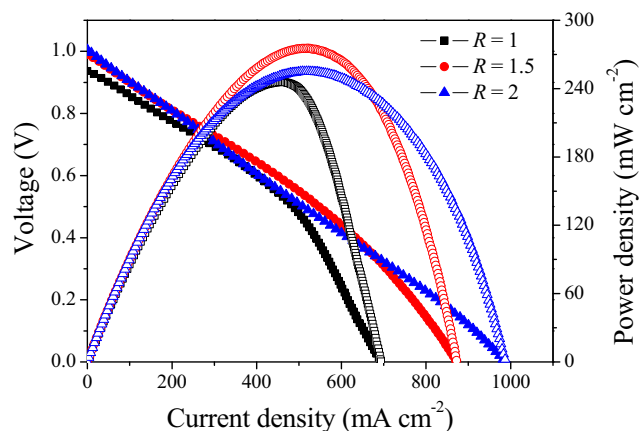


Fig. 2 *I-V* and *I-P* curves of the cell operated under traditional mode for various CH₄/O₂ ratios

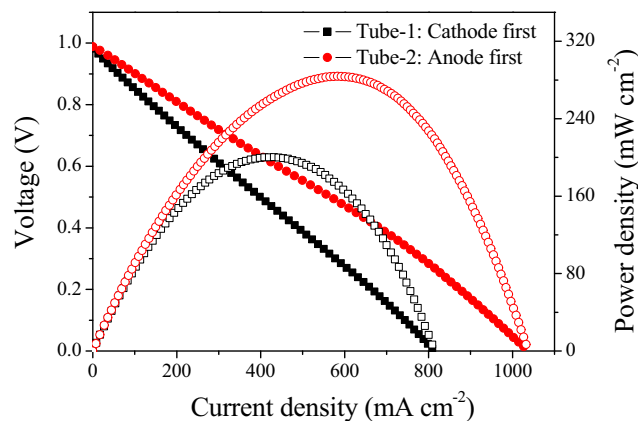


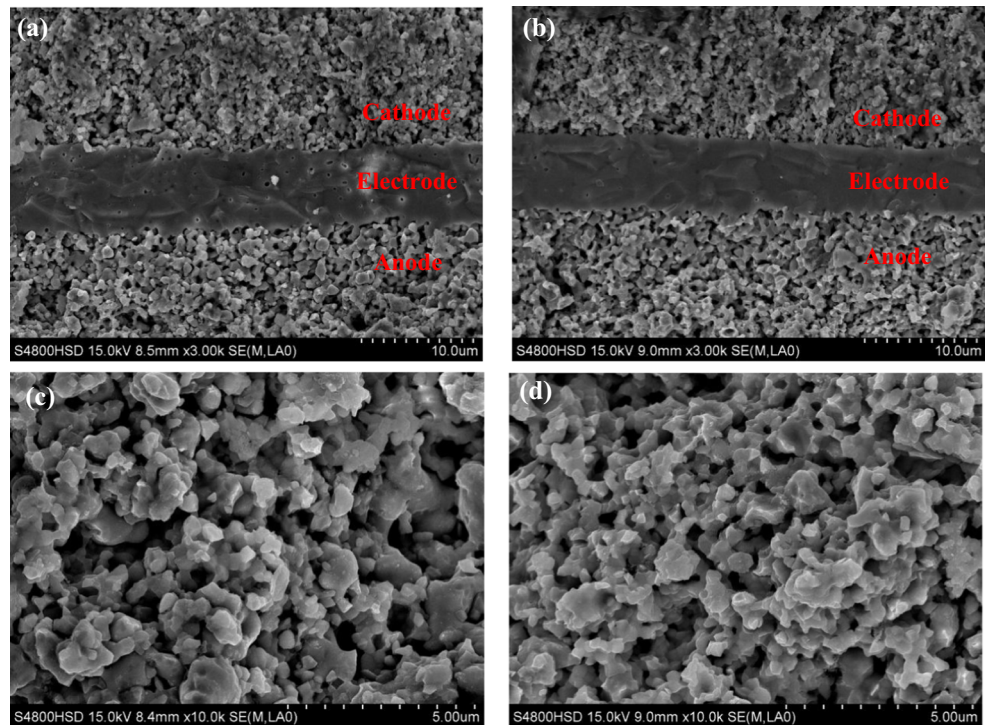
Fig. 3 *I-V* and *I-P* curves of the cathode-first and anode-first configurations at *R* = 1.5

presents the *I-V* and *I-P* curves of the cell at *R* = 1.5. The cell with anode-first configuration achieved a OCV of 0.99 V and a maximum power density of 283.7 mW cm⁻². The cathode-first configuration had a lower output power of 200 mW cm⁻². The measured temperature of the anode-first configuration was ~20 °C higher than that of the cathode-first configuration. Sufficient reactants were provided to the anode when the gas mixture reached first the anode side of the cell with tube 2. The heat evolved by methane oxidation caused an improved catalytic activity of anode, thus resulted in a higher output performance of the cell.

SEM images of the cells after cathode-first and anode-first configuration tests are shown in Fig. 4a, b. The YSZ electrolyte membranes were uniform and dense enough with a thickness of approximately 8 μm and adhered well to both the porous anode and cathode layers without showing any cracking or delamination. Layer interface was not observed between the electrodes and the films, ensuring a good stability of the cells. Microstructures of the anodes after the cell performance tests are shown in Fig. 4c, d. The SEM images showed very similar porous microstructures as expected for Ni/YSZ ceramics. No evidence of coke and nickel aggregation over the anodes was observed. Figure 5 shows the EDS spectra taken from the cross-section of Ni/YSZ anodes after different configuration tests. EDS spectra were also very similar, showing the expected Ni, Zr, O, and Y peaks. Very weak C peaks were present. There was little difference between the C peaks for cathode-first and anode-first configurations, suggesting that the C may have been from contamination in the SEM chamber.

Table 1 shows the effect of methane-oxygen ratio on OCV and maximum power density of the cell at 700 °C. The oxygen concentration gradients across the cell showed a strong dependence on the fuel-oxygen ratios. The highest output power appeared at *R* = 1.5 for both of the two configurations. Additionally, the maximum power density of the anode-first configuration was higher than that of the cathode-first

Fig. 4 Cross-section of the single cell and Ni/YSZ anode after different test conditions: **a** single cell of cathode-first configuration, **b** single cell of anode-first configuration, **c** anode of cathode-first configuration, and **d** anode of anode-first configuration



configuration, which was contrary to that obtained by the previous studies tested under the traditional gas supply mode [27, 33]. The gas supply methods with different flow geometries possess a significant influence on the cell performance. For the traditional cells, the lowest performance obtained in the cell configuration with the anode exposed to the gas flow, which was explained by the oxygen consumption before the gas mixture reached the cathode. Because of the open tube configuration of the traditional gas chamber [27], most of the reactant gas diffuses outside of the gas chamber directly without participating in the cathode reaction. The oxygen of

the cathode is seriously insufficient. However, the gas flow geometry is totally different for the anode-first configuration using tube 2. The reactive mixture reaches the cathode along the circular tube wall after passing over the anode. The reactants at the cathode are less affected compared with the traditional structure. Meanwhile, the circular tube wall is conducive to the heat accumulation around the cell. Therefore, the cell temperature is improved. Additionally, the gas vent at the side of the cell could shorten the transmission path of the gas flows to the surface of the anode, which would help to the diffusion of the reactant gas into the electrode, results in the good electrochemical and catalytic properties of the anode. As a result, the output power of the anode-first configuration using tube 2 was more than 2 times higher than that of the previous results [33].

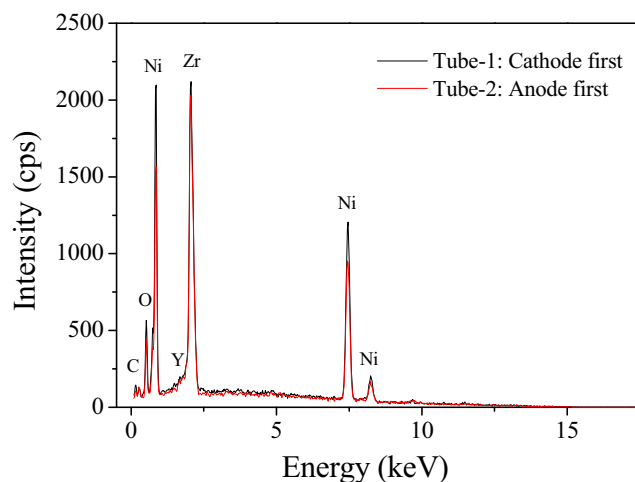


Fig. 5 EDS spectra taken from the cross-section of Ni/YSZ anodes after different test conditions

According to the operation mechanism of SC-SOFCs, the anode and cathode have different catalytic activities towards the fuel-oxygen mixture. The relative positioning of the electrodes in regard to the incoming gas flow should be optimized for both electrodes. In this study, the gas supply method with tube 1 and tube 2 could transmit reactant gas for cathode and anode separately, or for two electrodes simultaneously. The performance of the cell supplied with dual gas tubes has been studied herein. Under the dual gas supply mode, the gas mixture was evenly distributed into two gas paths. N_2 was still used as a diluted gas at a fixed flow rate of 100 sccm for each gas path. The total flow rate of CH_4 and O_2 through each gas path was 100 sccm, and the methane-oxygen ratio of the two gas paths was the same during the testing process. The output

Table 1 The effect of methane-oxygen ratio on OCV and maximum power density of the cell

700 °C, N ₂ = 200 sccm		R = 1	R = 1.5	R = 2
Tube 1: cathode-first configuration	OCV (V)	0.95	0.98	0.98
	Maximum power density (mW cm ⁻²)	173.4	200	187.7
Tube 2: anode-first configuration	OCV (V)	0.94	0.99	0.97
	Maximum power density (mW cm ⁻²)	236.7	283.7	234.7

performance of the cell for various CH₄/O₂ ratios is shown in Fig. 6. The OCV of the cell was above 1 V, higher than that of the traditional method. The maximum power densities were 406.1, 459.2, and 293.9 mW cm⁻² at R = 1, 1.5, and 2, respectively. The performance of the cell was obviously improved compared with the anode-first and cathode-first configurations supplied by only one gas tube. Both the anode and cathode of the cell could obtain reactants expeditiously and simultaneously using dual gas supply method. The problem of gas inadequacy at the opposite electrode side of tube 1 or tube 2 was solved.

The maximum power density of the dual gas supply method obtained at R = 1.5 (459.2 mW cm⁻²) was 67% higher than that of the traditional gas supply method (275.5 mW cm⁻²). The concentration polarization at high current at R = 1 was weakened substantially. The maximum current density increased from 693.9 mA cm⁻² of the traditional mode to 1369.4 mA cm⁻² of the dual gas supply mode at R = 1. It is illustrated that the dual gas supply method could better satisfy the demand of electrodes for gas composition. In the usual SC-SOFC gas supply mode, the reactant gas diffuses to the surface of electrodes to participate in reaction. Although the cell is located in the middle of the gas chamber as far as possible, it is difficult to ensure that the gas flow is uniformly distributed throughout the electrodes. While in a dual gas supply method, the gas mixture is evenly divided into two gas tubes and transports to the surfaces of the cathodes and anodes separately by their own gas vents. The direction of the gas flow is

perpendicular to the electrodes and the reaction gas is sprayed onto the surface of the anodes and cathodes directly, which

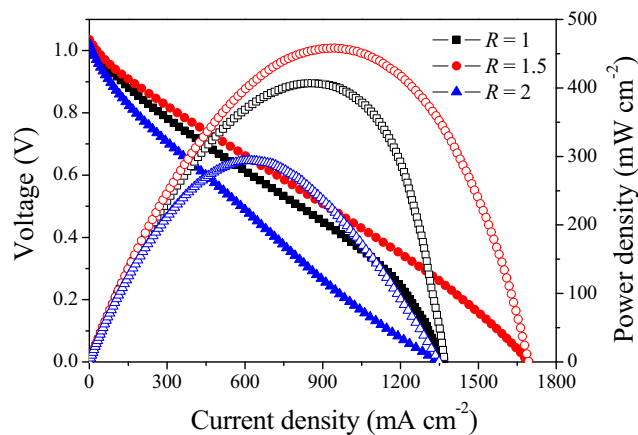


Fig. 6 *I-V* and *I-P* curves of the cell operated under dual gas supply method for various CH₄/O₂ ratios

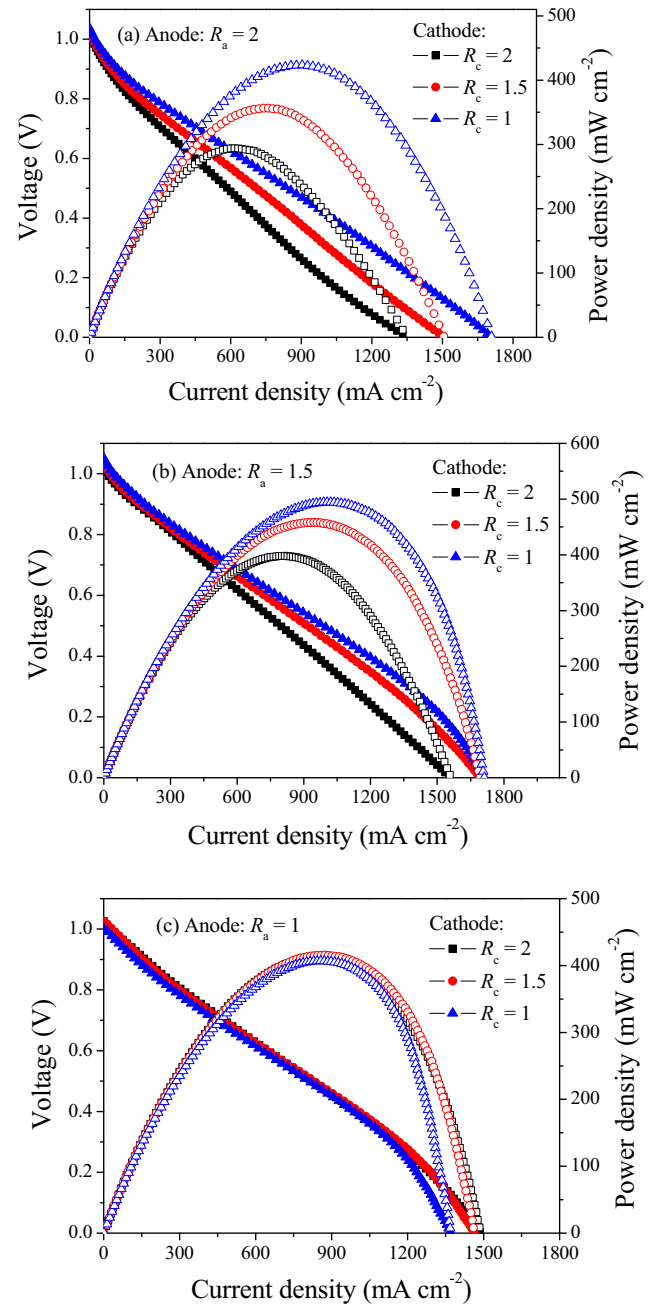


Fig. 7 The *I-V* and *I-P* curves of the cell with various CH₄/O₂ ratios being fed to the electrodes

Table 2 The output performance of the cell with various CH₄/O₂ ratios at both the electrodes

Dual gas supply method at 700 °C		$R_c = 1$	$R_c = 1.5$	$R_c = 2$
$R_a = 2$	OCV (V)	1.04	1.02	1.01
	Maximum power density (mW cm ⁻²)	422.4	355.1	293.9
$R_a = 1.5$	OCV (V)	1.05	1.03	1.01
	Maximum power density (mW cm ⁻²)	493.9	459.2	397.9
$R_a = 1$	OCV (V)	1.01	1.02	1.02
	Maximum power density (mW cm ⁻²)	406.1	414.3	412.2

ensures sufficient gas supplied for the electrodes. As a result, the cell performance has been promoted obviously.

Due to the different catalytic activity of the anode and cathode towards the fuel-oxygen mixture, the gas composition at the anode and cathode has a strong influence on the electrochemical properties of the respective electrodes. Oxygen-rich gas will be benefit for the cathode, while the anode needs to be provided fuel-rich gas. The dual gas supply method could provide required reactant gas for each electrode by changing the gas composition of the two gas tubes separately. The *I-V* and *I-P* curves of the cell with various CH₄/O₂ ratios being fed to both of the electrodes are shown in Fig. 7. R_a represents the CH₄/O₂ ratio at the anode side and R_c represents the CH₄/O₂ ratio at the cathode side. When R_a was fixed at 2 in Fig. 7a, the OCVs of 1.04, 1.02, and 1.01 V were obtained at $R_c = 1, 1.5,$ and $2,$ respectively. A decrease of OCV also occurred with the increase of R_c at $R_a = 1.5.$ Increasing the cathode gas ratio resulted in a lower oxygen concentration at the cathode and a reduction in OCV. The variety of OCV with R_c was not obvious at $R_a = 1$ where the oxygen concentration at the anode side increased.

Detailed data of the cell performance is shown in Table 2. The maximum power density of the cell decreased with increasing R_c at both the anode CH₄/O₂ ratios of 1.5 and 2. It is proved that increasing the oxygen concentration at the cathode side promotes the electrochemical reduction reaction rate of oxygen. The cathode gas ratio of 1 was found the optimum ratio. The highest power density of 493.9 mW cm⁻² was obtained at $R_a = 1.5$ and $R_c = 1.$ Besides, a slight concentration polarization was observed at high current part. When the CH₄/O₂ ratio at the anode was fixed at 1, the maximum power densities remained almost constant with various R_c and showed a mild decrease at $R_c = 1,$ the same with the trend of OCV. Furthermore, all the *I-V* curves exhibited concentration polarization phenomenon at $R_a = 1,$ which indicated that excessive oxygen at the anode was inappropriate. The complete oxidation of methane produced H₂O and CO₂, which do not participated in the electrochemical reaction of the cell, caused a degradation of the cell performance.

The impedance spectra of the cell measured under open circuit voltage condition are shown in Fig. 8. The electrode polarization resistances at $R_a = 2$ were 1.52, 1.63, and

1.73 Ω cm² when $R_c = 1, 1.5,$ and $2,$ respectively, which were increased with the increasing $R_c.$ It is obvious that the polarization resistance at $R_a = 1.5$ was lower than that at $R_a = 2,$ which indicated the improvement of the cell performance. The electrode polarization resistance was also increased with the increasing R_c at $R_a = 1.5.$ These results provided further evidence that the cathode CH₄/O₂ ratio of 1 was the optimal ratio for the cell performance. The electrode polarization resistances at $R_a = 1$ were nearly the same at various R_c as shown in Fig. 8c, which presented direct evidence of its consistent output power.

Figure 9 shows the maximum power density of the cell as a function of CH₄ flow rate at the anode side where the cathode CH₄/O₂ ratio R_c was fixed at 1. The total flow rate of CH₄ and O₂ was 100 sccm for each gas path. The maximum power density increased from 406.1 to 493.9 mW cm⁻² when the CH₄ flow rate changed from 50 to 60 sccm. It was then decreased gradually at higher CH₄ flow rates, which was probably caused by the decreasing of H₂ and CO produced by methane catalytic partial oxidation with decreased oxygen concentration in the gas mixture. The output power remained constant when CH₄ flow rate increased continuously from 90 to 100 sccm. It was shown that the anode and cathode gas ratios of 1.5 and 1 possessed the optimal gas composition for the cell performance. Based on our results, a cell with dual gas supply method will generate a more attractive output power than that of the traditional method in a single-chamber condition. Oxygen-rich gas is fed to the cathode and fuel-rich gas to the anode, without the need to separate the two electrode chambers. Thus, the selectivity requirement of both the anode and cathode for the fuel and oxygen in mixed gas has been lowered.

Fuel utilization as a function of the current density under different gas supply methods is shown in Fig. 10. The fuel utilization of traditional mode at the maximum current density was 0.62% at CH₄ flow rate of 120 sccm. Basically, there are three major factors responsible for the low efficiency of SC-SOFCs: poor flow management, non-ideal electrode microstructure, and low selectivity of the electrode materials [34]. With the fixed materials, electrode microstructures, and catalytic properties of a

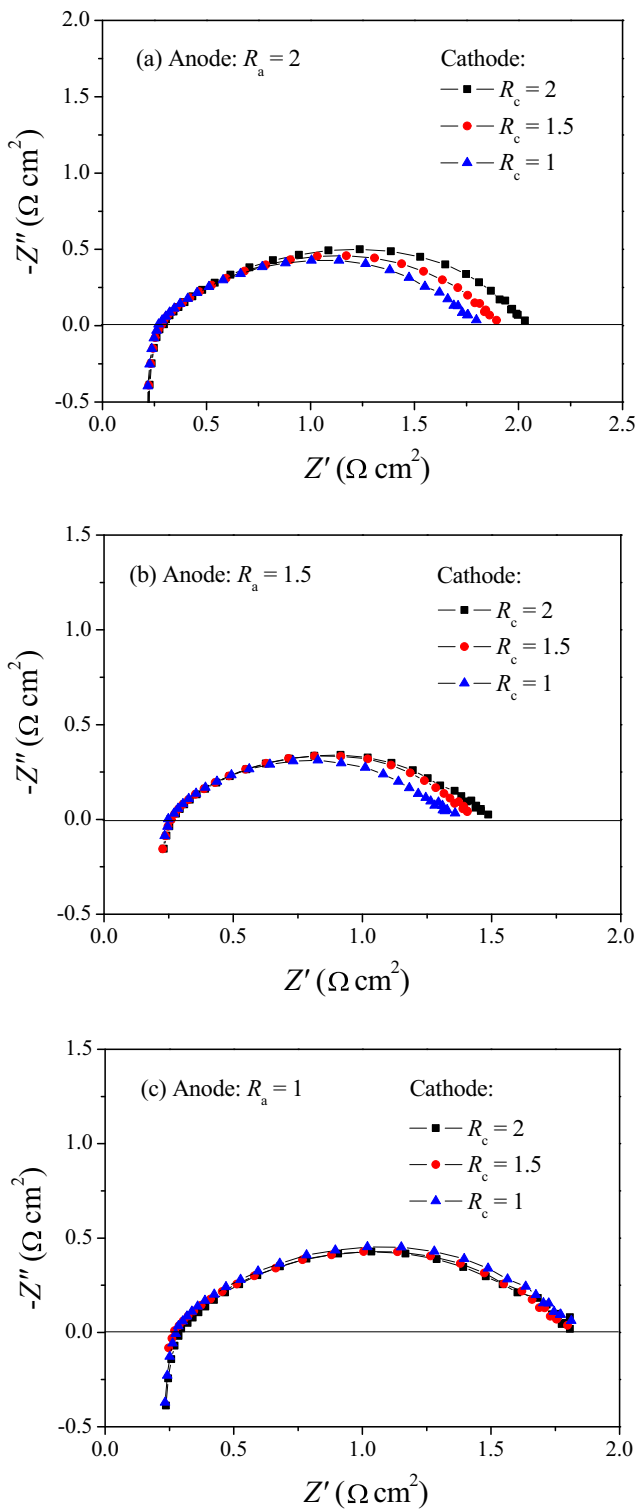


Fig. 8 Impedance spectra of the cell with various CH₄/O₂ ratios at both the electrodes

given cell, the improvement of the power generation essentially amounts to optimizing the distribution of the reactants around the cell, achievable through a careful management of the gas flow geometry in the gas chamber.

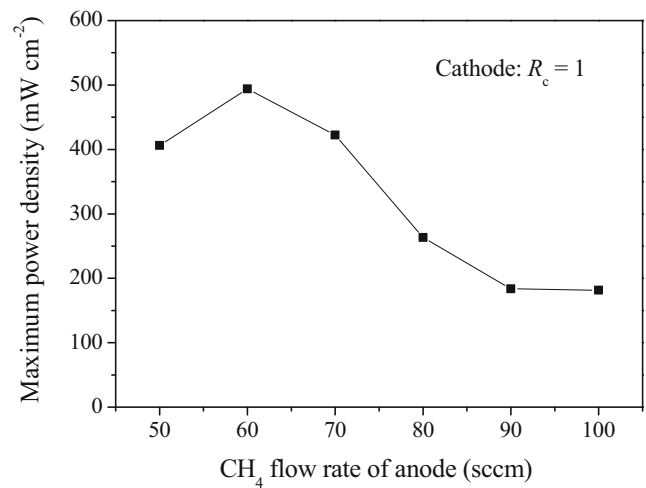


Fig. 9 The maximum power density of the cell as a function of CH₄ rate at the anode

In this study, dual gas supply method is used to enhance the efficiency of SC-SOFCs by improving the flow geometry. As shown in Fig. 10b, the dual gas supply method

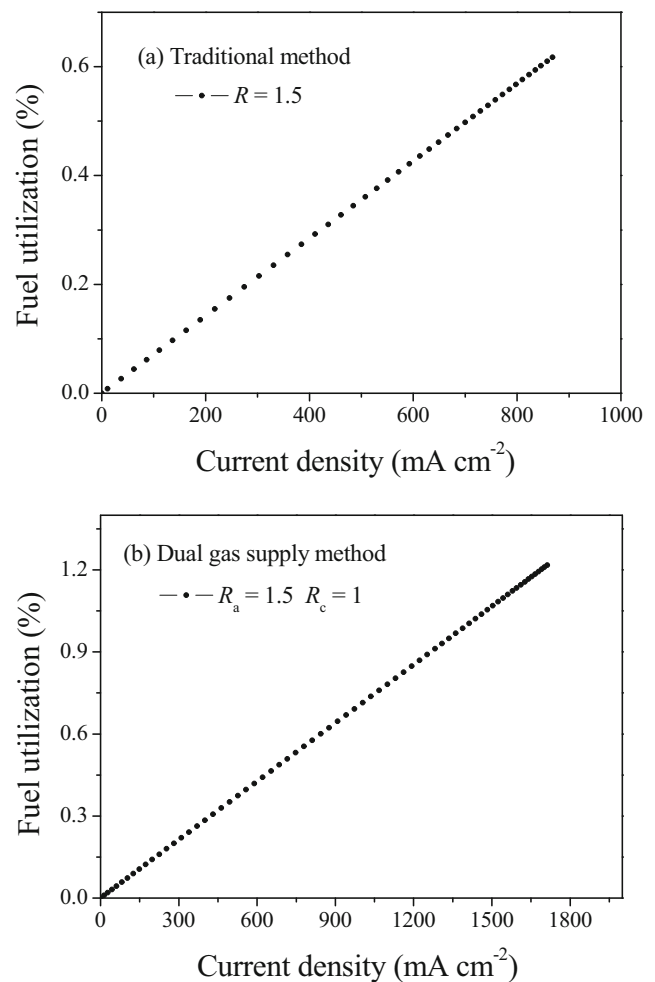


Fig. 10 Fuel utilization as a function of current density under different gas supply methods: **a** traditional mode and **b** dual gas supply method

possessed a fuel utilization of 1.22%, which was 2 times higher than the former one. The fuel utilization also increased with the increase of the residence time [11]. Therefore, a moderate gas flow rate should be used to obtain both high power output and acceptable fuel utilization. In addition, more cells can be placed in the same gas flow rate to improve the fuel utilization [19]. Our previous study of the separated gas supply method showed that the single cells could obtain a more uniform gas distribution and the stack could produce a higher power output than that of the traditional gas supply method [30]. It is expected to further improve the output performance and fuel utilization of the SC-SOFCs by using the dual gas supply method.

Conclusion

A single cell with dual gas supply method was fabricated and operated under single-chamber conditions. The performance of the anode-first and cathode-first configurations has also been studied. Results show that the maximum power of the anode-first configuration was higher than that of the cathode-first one, which was contrary to that obtained under the traditional gas supply method. The gas supply methods with different flow geometries have a significant influence on the cell performance.

The cell with dual gas supply method showed remarkably enhanced OCV and output performance compared with the traditional method. At a temperature of 700 °C and a CH₄/O₂ ratio of 1.5, the cell with dual gas supply method exhibited a maximum power density of 459.2 mW cm⁻², which was 67% higher than that of the traditional gas supply method. The highest power density of 493.9 mW cm⁻² was obtained at the anode and cathode gas ratios of 1.5 and 1, respectively, which were found the optimum gas ratios for the cell performance. Oxygen-rich gas is fed to the cathode and fuel-rich gas to the anode in the dual gas supply mode. The selectivity requirement of both the anode and cathode for the fuel and oxygen in mixed gas has been lowered.

Funding information This study was supported by the National Natural Science Foundation of China (Nos. 51602213, 11604236, and 61575139) and the Youth Foundation of the Taiyuan University of Technology (No. 2015QN071).

Compliance with ethical standards

Conflict of interest The authors declare that they have no conflict of interest.

Publisher's note Springer Nature remains neutral with regard to jurisdictional claims in published maps and institutional affiliations.

References

- Sun CW, Stimming U (2007) Recent anode advances in solid oxide fuel cells. *J Power Sources* 171:247–260
- Chen KF, Tian YT, Lü Z, Ai N, Huang XQ, Su WH (2009) Behavior of 3 Mol% yttria-stabilized tetragonal zirconia polycrystal film prepared by slurry spin coating. *J Power Sources* 186:128–132
- Sun CW, Xie Z, Xia CR, Li H, Chen LQ (2006) Investigations of mesoporous CeO₂-Ru as a reforming catalyst layer for solid oxide fuel cells. *Electrochem Commun* 8:833–838
- Yang W, Zhu CL, Ma ZH, Sun CW, Chen LQ, Chen YJ (2014) MoO₃ nanorods/Fe₂(MoO₄)₃ nanoparticles composite anode for solid oxide fuel cells. *Int J Hydrog Energy* 39:14411–14415
- Yang Q, Chai FT, Ma C, Sun CW, Shi SQ, Chen LQ (2016) Enhanced coking tolerance of MgO-promoted Ni cermet anode for hydrocarbon fueled solid oxide fuel cells. *J Mater Chem A* 4: 18031–18036
- Yang Q, Chen J, Sun CW, Chen LQ (2016) Direct operation of methane fueled solid oxide fuel cells with Ni cermet anode via Sn modification. *Int J Hydrog Energy* 41:11391–11398
- Kuhn M, Napporn TW (2010) Single-chamber solid oxide fuel cell technology - from its origins to Today's state of the art. *Energies* 3: 57–134
- Wei B, Lu Z, Huang XQ, Liu ML, Chen KF, Su WH (2007) Enhanced performance of a single-chamber solid oxide fuel cell with an SDC-impregnated cathode. *J Power Sources* 167:58–63
- Buegler BE, Siegrist ME, Gauckler LJ (2005) Single chamber solid oxide fuel cells with integrated current-collectors. *Solid State Ionics* 176:1717–1722
- Yano M, Tomita A, Sano M, Hibino T (2007) Recent advances in single-chamber solid oxide fuel cells: a review. *Solid State Ionics* 177:3351–3359
- Riess I (2008) On the single chamber solid oxide fuel cells. *J Power Sources* 175:325–337
- Yano M, Nagao M, Okamoto K, Tomita A, Uchiyama Y, Uchiyama N, Hibino T (2008) A single-chamber SOFC stack operating in engine exhaust. *Electrochem Solid-State Lett* 11:B29–B33
- Shao ZP, Mederos J, Chueh WC, Haile SM (2006) High power-density single-chamber fuel cells operated on methane. *J Power Sources* 162:589–596
- Hibino T, Hashimoto A, Inoue T, Tokuno JI, Yoshida SI, Sano M (2000) Single-chamber solid oxide fuel cells at intermediate temperatures with various hydrocarbon-air mixtures. *J Electrochem Soc* 147:2888–2892
- Tomita A, Hirabayashi D, Hibino T, Nagao M, Sano M (2005) Single-chamber SOFCs with a Ce_{0.9}Gd_{0.1}O_{1.95} electrolyte film for low-temperature operation. *Electrochem Solid-State Lett* 8-1:A63–A65
- Yano M, Kawai T, Okamoto K, Nagao M, Sano M, Tomita A, Hibino T (2007) Single-chamber SOFCs using dimethyl ether and ethanol. *J Electrochem Soc* 154:B865–B870
- Napporn TW, Jacques-Bédard X, Morin F, Meunier M (2004) Operating conditions of a single-chamber SOFC. *J Electrochem Soc* 151:A2088–A2094
- Shao ZP, Kwak C, Haile SM (2004) Anode-supported thin-film fuel cells operated in a single chamber configuration 2T-I-12. *Solid State Ionics* 175:39–46
- Suzuki T, Jasinski P, Petrovsky V, Anderson HU, Dogan F (2004) Anode supported single chamber solid oxide fuel cell in CH₄-air mixture. *J Electrochem Soc* 151:A1473–A1476
- Suzuki T, Jasinski P, Petrovsky V, Anderson HU, Dogan F (2005) Performance of a porous electrolyte in single-chamber SOFCs. *J Electrochem Soc* 152:A527–A531

21. Napporn TW, Morin F, Meunier M (2004) Evaluation of the actual working temperature of a single-chamber SOFC. *Electrochem Solid-State Lett* 7:A60–A62
22. Shao ZP, Haile SM, Ahn J, Ronney PD, Zhan ZL, Barnett SA (2005) A thermally self-sustained micro solid-oxide fuel-cell stack with high power density. *Nature* 435:795–798
23. Hibino T, Hashimoto A, Inoue T, Tokuno JI, Yoshida SI, Sano M (2001) A solid oxide fuel cell using an exothermic reaction as the heat source. *J Electrochem Soc* 148:A544–A549
24. Hibino T, Hashimoto A, Yano M, Suzuki M, Yoshida S, Sanob M (2002) High performance anodes for SOFCs operating in methane-air mixture at reduced temperatures. *J Electrochem Soc* 149:A133–A136
25. Zhang CM, Sun LL, Ran R, Shao ZP (2009) Activation of a single-chamber solid oxide fuel cell by a simple catalyst-assisted in-situ process. *Electrochem Commun* 11:1563–1566
26. Bay L, Horita T, Sakai N, Ishikawa M, Yamaji K, Yokokawa H (1998) Hydrogen solubility in Pr-doped and un-doped YSZ for a one chamber fuel cell. *Solid State Ionics* 113-115:363–367
27. Stefan IC, Jacobson CP, Visco SJ, De Jonghe LC (2004) Single chamber fuel cells: flow geometry, rate, and composition considerations. *Electrochem Solid-State Lett* 7:A198–A200
28. Morel B, Roberge R, Savoie S, Napporn TW, Meunier M (2009) Temperature and performance variations along single chamber solid oxide fuel cells. *J Power Sources* 186:89–95
29. Jacques-Bédard X, Napporn TW, Roberge R, Meunier M (2007) Coplanar electrodes Design for a Single-Chamber SOFC assessment of the operating parameters. *J Electrochem Soc* 154:B305–B309
30. Tian YT, Lü Z, Liu ML, Zhu XB, Wei B, Zhang YH, Huang XQ, Su WH (2013) Effect of gas supply method on the performance of the single-chamber SOFC micro-stack and the single cells. *J Solid State Electrochem* 17:269–275
31. Wei B, Lü Z, Huang XQ, Liu ML, Jia DC, Su WH (2009) A novel design of single-chamber SOFC micro-stack operated in methane-oxygen mixture. *Electrochem Commun* 11:347–350
32. Liu ML, Lü Z, Wei B, Huang XQ, Chen KF, Su WH (2009) A novel cell-Array Design for Single Chamber SOFC microstack. *Fuel Cells* 9(5):717–721
33. Liu ML, Qi X, Lv Z, Meng QY (2013) Effect of flow geometry on anode-supported single chamber SOFCs arrayed as V-shape. *Int J Hydrog Energy* 38:1976–1982
34. Hao Y, Goodwin DG (2008) Efficiency and fuel utilization of methane-powered single-chamber solid oxide fuel cells. *J Power Sources* 183:157–163